Relations between the quasi-biweekly oscillation over the East Asian monsoon region and the East Asian tropical monsoon depressions

Jingyi Li[1,2], Min Wen*[2], Zunya Wang[3], and Yi Hu[4]

[1] Anhui Meteorological Observatory, Hefei 230031

[2] State Key Laboratory of Severe Weather, Chinese Academy of Meteorological Sciences, Beijing 100081, China

[3] National Climate Center, China Meteorological Administration, Beijing 100081, China

[4] National Meteorological Center, China Meteorological Administration, Beijing 100081, China

* Corresponding author’s E-mail: wenmin@cma.gov.cn

Funding information: National Natural Science Foundation of China (Grant 41775060) and National Key Research and Development Program of China, Grant/Award Number:2016YFA0600602

Published journal: Li J Y, Wen M, Wang Z Y, Hu Y. Relations between the quasi-biweekly oscillation over the East Asian monsoon region and the East Asian tropical monsoon depressions. International Journal of Climatology: A Journal of the Royal Meteorological Society, 2021, 41(2):878-895.

Keywords: convection, East Asian tropical monsoon depression, quasi-biweekly oscillation, Western Pacific subtropical high

In addition to synoptic disturbances, the 10–20 day oscillation (QBWO) is a dominant sub-seasonal oscillation signal of convection in tropical East Asia during the boreal summer, especially in the South China Sea (SCS) (Fig.1). This result is consistent with previously reported studies (Chen and Sui, 2010; Jia and Yang, 2013).The first two leading modes of an empirical orthogonal function (EOF) analysis to a 34-year series of daily 10–20 day filtered outgoing longwave radiation (OLR) anomalous data over tropical East Asia showed a north-westward propagating mode of the quasi-biweekly oscillation (QBWO) (Fig.2). The original signal of this convective QBWO mode was present over the tropical central Pacific near 180° and then propagated north-westward. The signal enhanced during propagation and then disappeared as it made landfall. The active centre of convection of the QBWO coincided with a positive potential vorticity (PV) anomaly at 500 hPa and a cyclonic gyre at 850 hPa, whereas the centre of suppression coincided with a negative PV anomaly and an anticyclonic gyre. These circulations made up an inclined northwest-southeast wave train (Fig.3).

The vertical structures of this dominant QBWO mode show that the vertical dynamic and thermodynamic structures of the QBWO mode have many similarities with those of East Asian tropical monsoon depressions (EAMDs). Both structures have two centres of PV at 500 and 750 hPa, respectively, and have an almost upright structure in the troposphere up to 300 hPa (Hurley and Boos, 2015; Hu et al.,2019) (shadings of Fig.4). The low-level centre of relative vorticity anomalies is located at 850 hPa, lower than that of the PV. At most times, the low-level centre is stronger than the centre at 500 hPa, which resembles the relative vorticity structure of EAMDs (Hu et al.,2019) (contours of Fig.4). The convective cell of the QBWO has a warm-over-cold structure in the troposphere, which resembles that of EAMDs (Hu et al.,2019) (contours in the left-hand column of Fig.5). These similarities may imply a close relationship between the QBWO and EAMDs.

The location of the EAMDs in each phase of the QBWO mode were investigated and found that EAMDs are more likely to appear in a region of strong convection. When the cyclonic circulation corresponding to the region of active convection is sufficiently strong, the EAMDs are more likely to appear in the cyclonic circulation and move north-westward together with the cyclonic circulation (Fig.6 and Fig.7). Based on the relationship between the QBWO and the location of EAMDs, we can infer that some structure information of EAMDs is projected onto the signal identified as that of the QBWO. However, it cannot change the structure of the QBWO significantly because their scales differ in magnitude.

We also explored QBWO modulation at different stages of the EAMDs and in different track groups. The EAMDs are preferentially generated over regions of deep convection. (Table 1 and Fig.8). Boos et al. (2015) suggested that the horizontal adiabatic advection of PV at 500 hPa causes the Indian monsoon depression to move westward against the westerly winds at lower levels. Hu et al. (2019) showed that the maximum PV centre of EAMDs is also located at 500 hPa, the same as for the Indian monsoon depression. The unfiltered 500 hPa circulation shows that the westernmost point of the Western Pacific subtropical high (WPSH) reaches west to 100° E in phase 1 (Fig.9). As a result, all the EAMDs generated in this phase are located in the easterlies to the south of the WPSH. The composite unfiltered 500 hPa circulation in the following phases shows that the easterlies are maintained for a long time. Therefore, the EAMDs move westward under the influence of the horizontal adiabatic advection of the PV. The anomalous anticyclone becomes weak from phases 4 to 7 as it nears land and disappears in phase 5, whereas the anomalous cyclone associated with convection over the western North Pacific (WNP) is enhanced. This suggests that the WPSH weakens and retreats eastward (Fig.9), and therefore, many eastward-moving EAMDs are generated in these phases in addition to westward and northwestward-moving EAMDs (Table 1).

Figure 10 shows the location of the EAMDs when they reach their strongest vorticity in the eight phases of the QBWO. Most of the EAMDs reach their peak intensity when they move over the SCS, and the number of EAMDs occurring in the region of active convection is higher than that occurring in the region of suppressed convection. They are 76 and 44, respectively. This indicates that vigorous convection favours the enhancement of EAMDs. However, there is no significant relation between the QBWO convection and the point of disappearance of EAMDs. The decay of EAMDs is primarily related to friction with the ground surface, the transport of moisture and the heat supply (Liu and Liang,1988) (Fig.11).

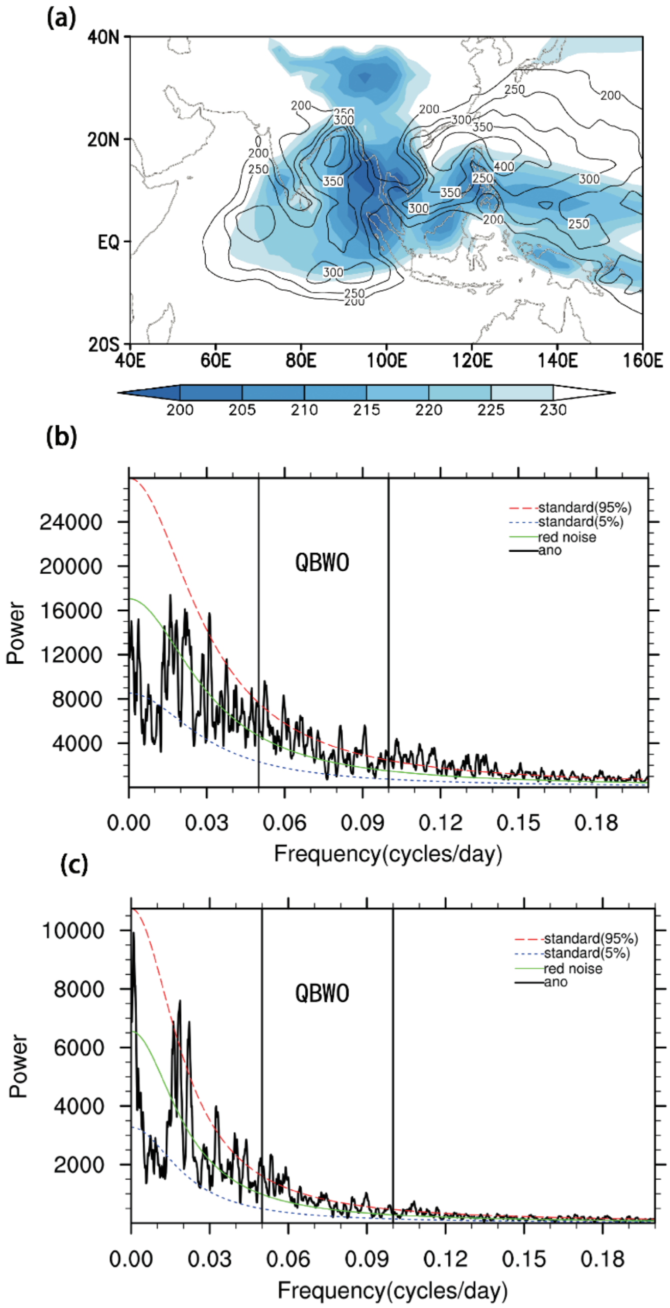

Fig. 1 (a) Climatological (1979－2012) patterns of the May to October OLR (blue shading in units of W m^{-2}) and variance of the 10－20 day filtered OLR (black contours in units of (W m^{-2})^{2}). Power spectra of the OLR anomalies (thick lines) averaged over the (b) SCS (10° －20° N, 110° －120° E) and (c) WNP (10° －20° N, 120° －160° E). The thin green dashed lines show the spectral density of red noise and thin red solid lines and blue dotted lines are the 95% confidence bounds of the red noise.

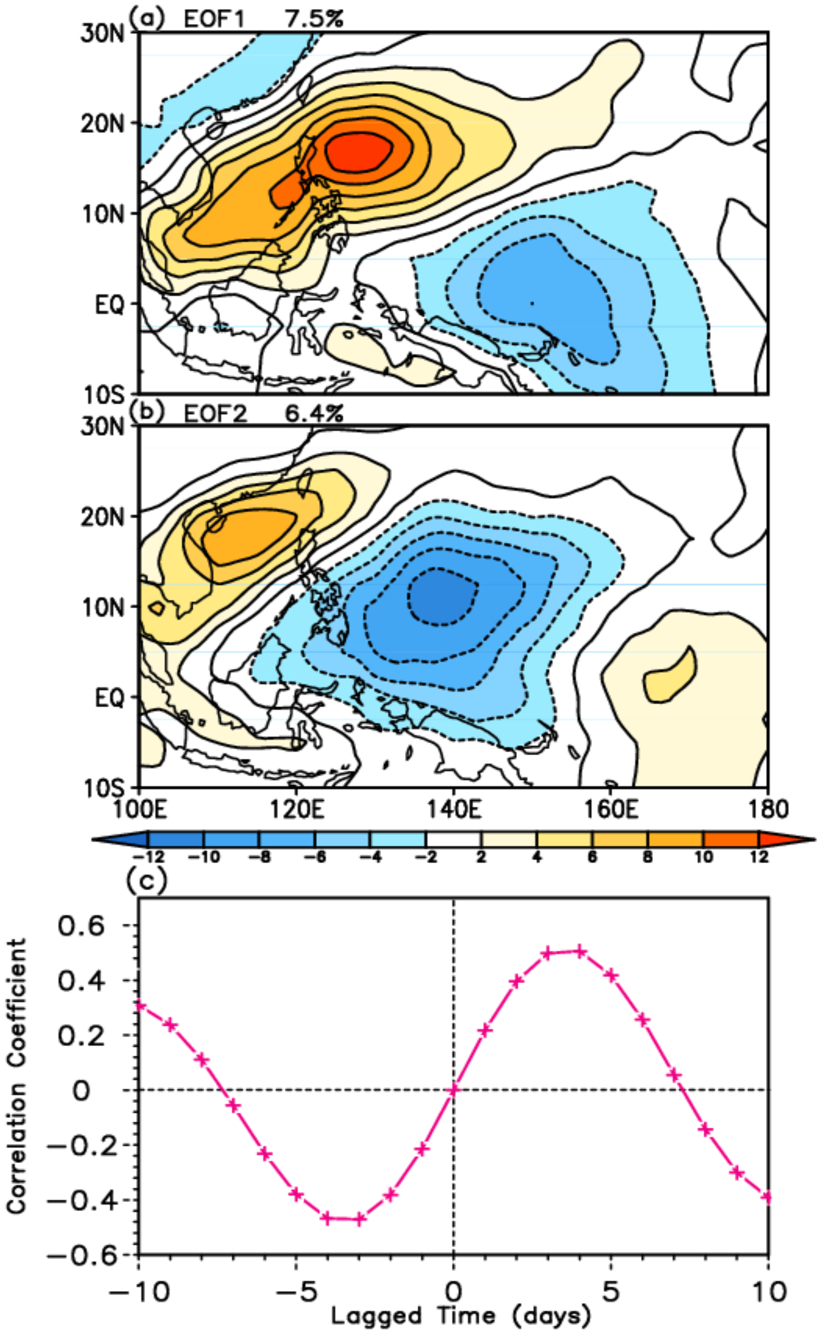

Fig. 2 Patterns of the (a) first and (b) second EOF modes of the 10-20 day filtered OLR (W m^{-2}), and (c) the correlation coefficients of the principal components for May-October during the period 1979-2012.

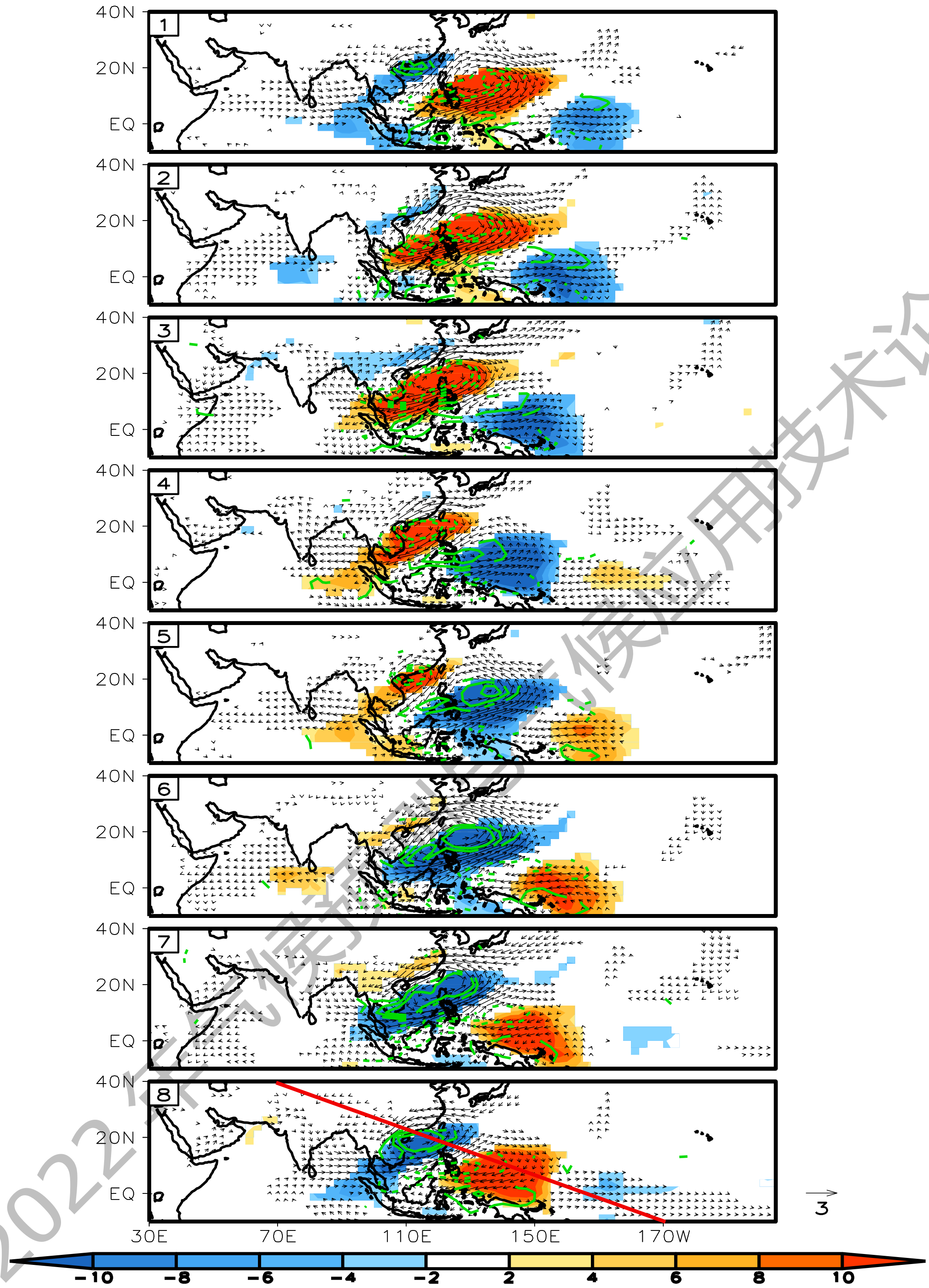

Fig. 3 Composite 10 - 20 day 850 hPa winds (vectors in units of m s^{-1}), OLR anomalies (shadings in units of W m^{-2}) and 500 hPa PV (contours in units of 10^{-2} PVU, where 1 PVU = 10^{-6} K m^2 kg^{-1} s^{-1}) in the eight phases of the QBWO. The red line in phase 8 indicates the vertical cross-section along the inclined axis of the wave train.

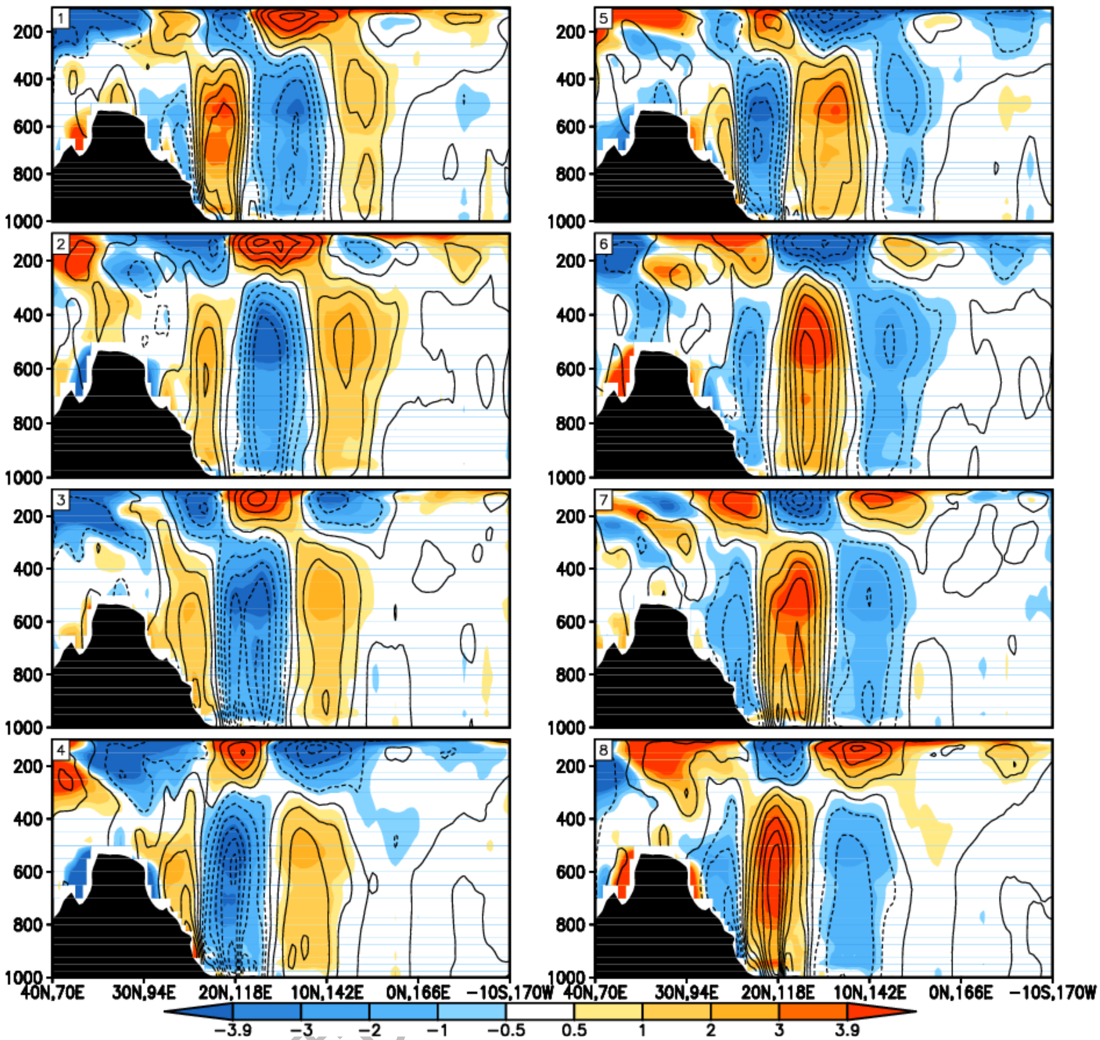

Fig. 4 Cross-sections of the composite 10 - 20 day PV (shadings in units of 10^{-2} PVU, where 1 PVU $=10^{-6}$ K m^2 kg^{-1} s^{-1}) and relative vorticity (contours in units of $10^{-6}s^{-1}$) from (40° N, 70° E) to (10° S, 170° W) in the eight phases of the QBWO.

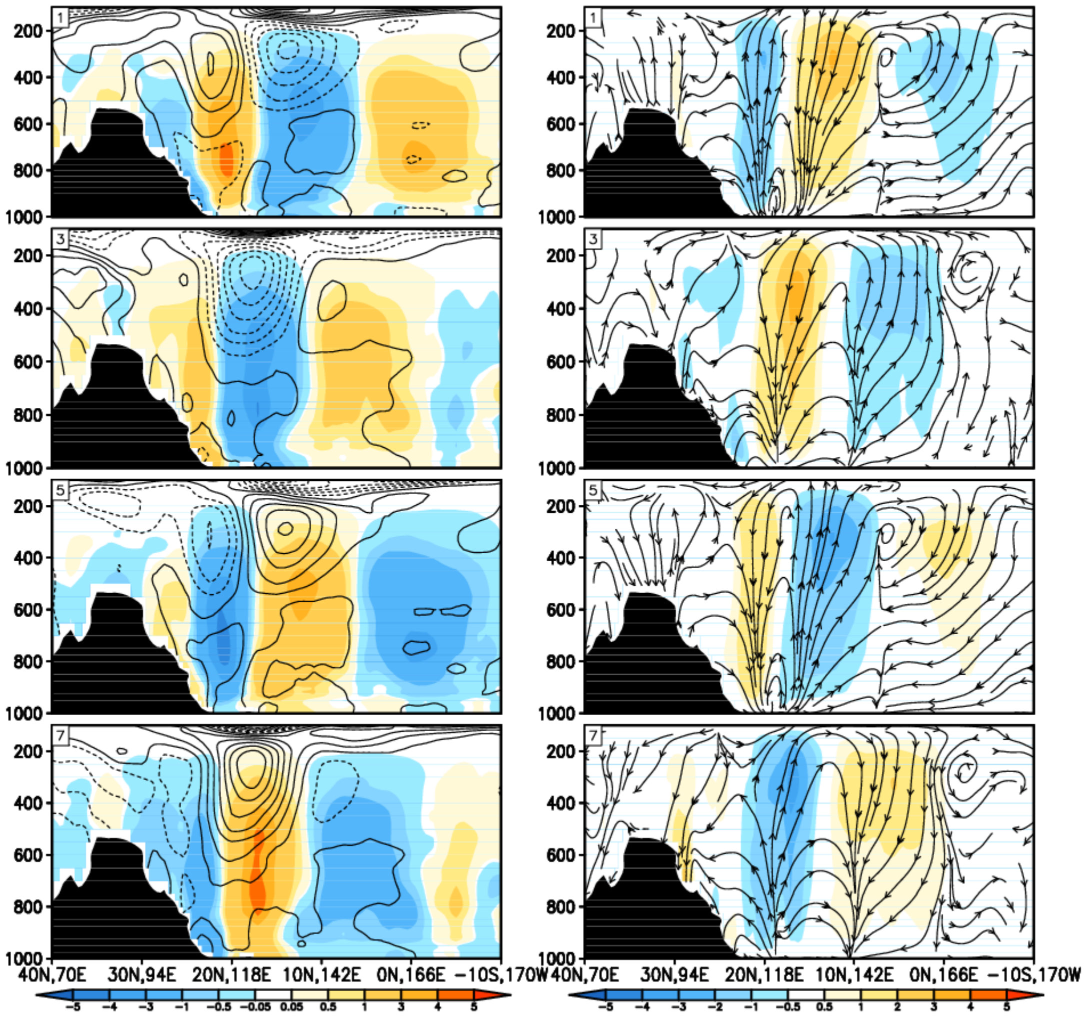

Fig. 5 Cross-sections of the composite 10 - 20 day specific humidity (shadings in units of 10^{-1}kg kg^{-1}) and potential temperature (contours in units of 10^{-1}K) from (40° N, 70° E) to (10° S, 170° W) (left-hand column), and vertical velocity (shadings in units of 10^{-2} Pa/s) and vertical circulation (streamline) (right-hand column) in the phases 1, 3, 5, and 7 of the QBWO.

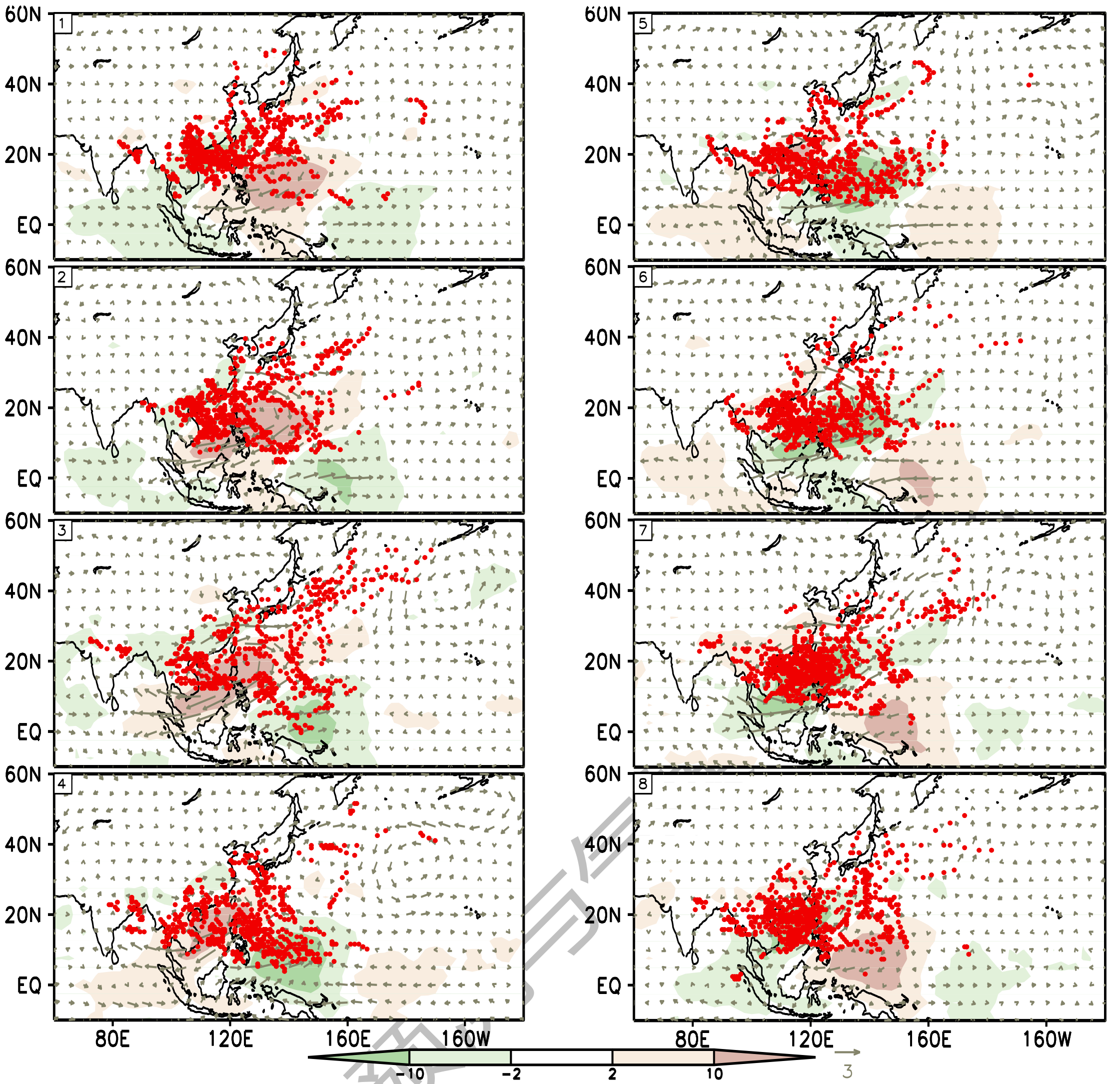

Fig. 6 Locations of all EAMDs at all times (dots), composite 10-20 day filtered 500 hPa anomalous winds (vectors in units of m s^{-1}) and OLR anomalies (shading in units of W m^{-2}) in the eight phases of the QBWO.

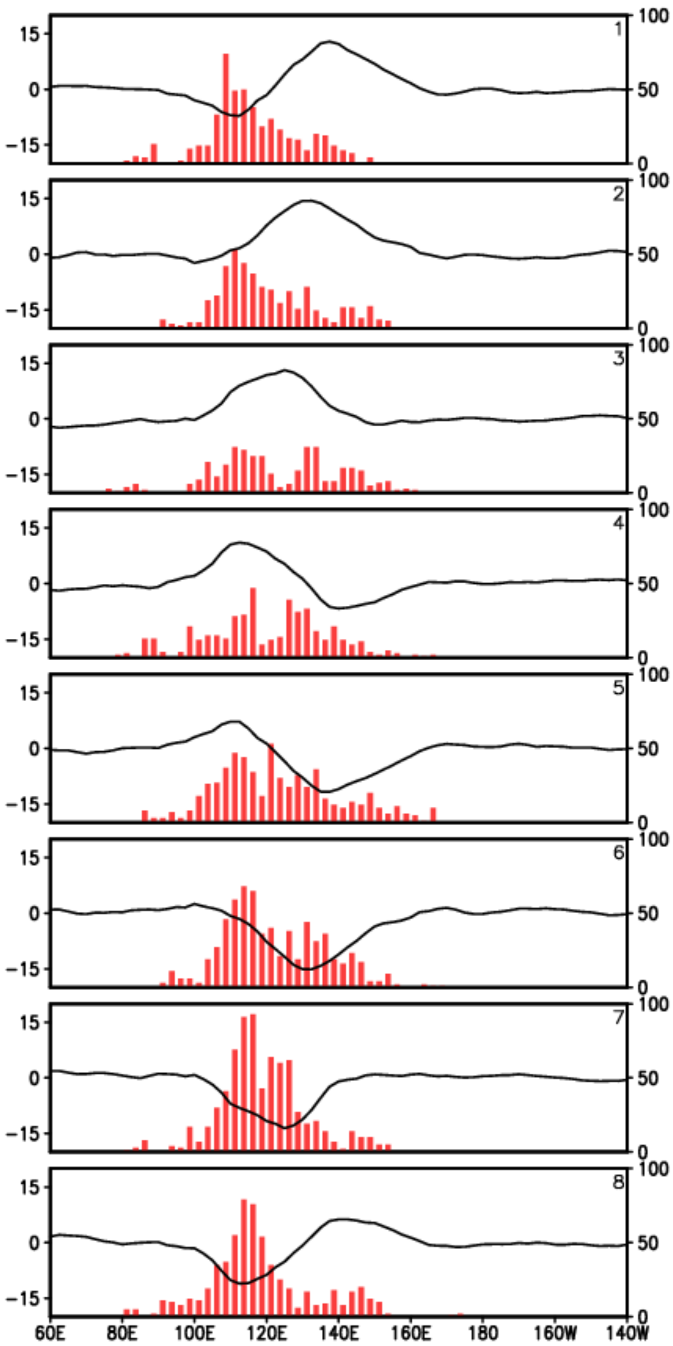

Fig. 7 Numbers of EAMDs at all times (red bar, corresponding to right-hand axis) and averaged 10－20 day filtered OLR anomalies (black curve, corresponding to left-hand axis) in 10°－25°N in the eight phases of the QBWO.

Table 1 Numbers and percentages of the genesis of EAMDs in different OLR values in eight phases of the QBWO.

	eastward-moving	westward-moving	northwestward-moving	turning	sum	
	number of EAMDs (percent)	number of EAMDs (percent)	number of EAMDs (percent)	number of EAMDs (percent)	OLR<0 number of EAMDs	OLR>0 number of EAMDs
Phase1	**0(0.0)**	**6(54.5)**	**4(36.4)**	**1(9.1)**	**5**	**6**
Phase2	**2(11.8)**	**5(29.4)**	**4(23.5)**	**6(35.3)**	**3**	**14**
Phase3	**0(0.0)**	**6(40.0)**	**6(40.0)**	**3(20.0)**	**10**	**5**
Phase4	**7(35.0)**	**5(25.0)**	**4(20.0)**	**4(20.0)**	**13**	**7**
Phase5	**2(10.5)**	**8(42.1)**	**4(21.1)**	**5(26.3)**	**13**	**6**
Phase6	**3(37.5)**	**1(12.5)**	**2(25.0)**	**2(25.0)**	**7**	**1**
Phase7	**4(25.0)**	**5(31.3)**	**4(25.0)**	**3(18.8)**	**12**	**4**
Phase8	**1(8.3)**	**5(41.7)**	**2(16.7)**	**4(33.3)**	**4**	**8**

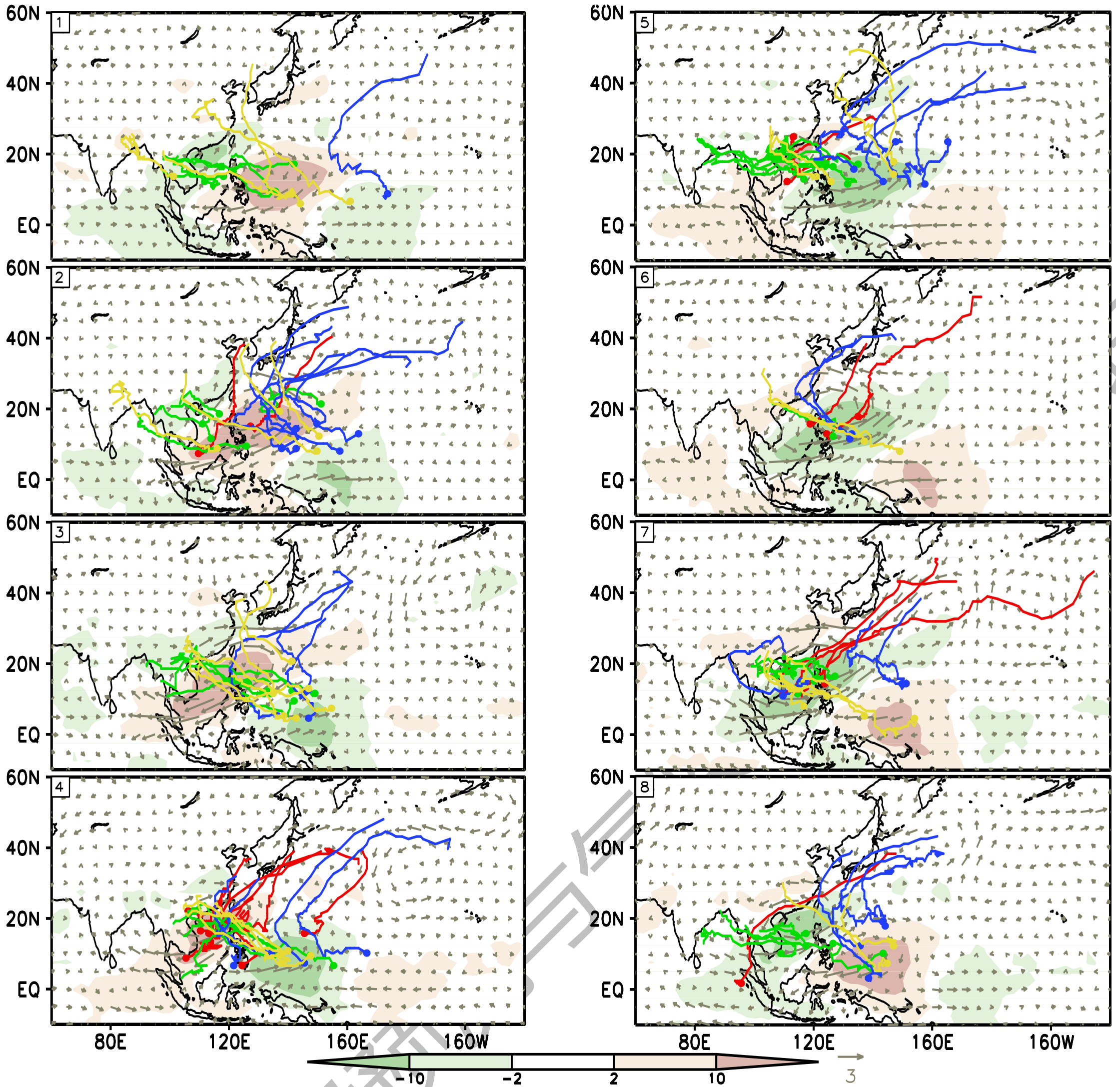

Fig. 8 Locations of the genesis of EAMDs and tracks after the genesis times (dots and lines), composite 10-20 day filtered 500 hPa anomalous winds (vectors) and OLR anomalies (shading) in the eight phases of the QBWO. The red dots and lines are the genesis locations and tracks of eastward-moving EAMDs, the green dots and lines are those of westward-moving EAMDs, the yellow dots and lines are those of northwestward-moving EAMDs and the blue dots and lines are those of turning EAMDs.

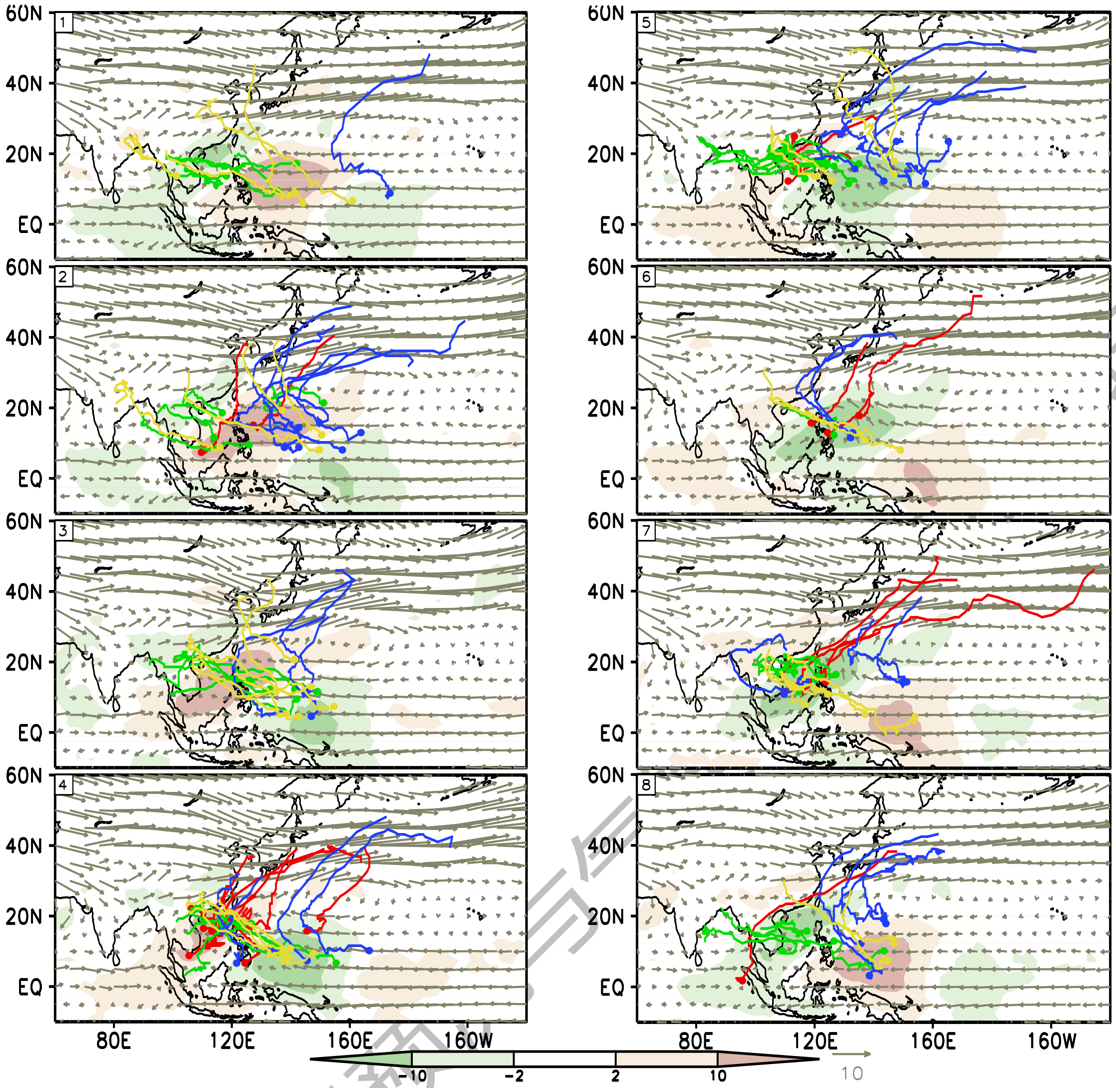

Fig. 9 Locations of the genesis of EAMDs and tracks after the genesis times (dots and lines), composite 10-20 day unfiltered 500 hPa winds (vectors) and OLR anomalies (shading) in the eight phases of the QBWO. The red dots and lines are the genesis locations and tracks of eastward-moving EAMDs, the green dots and lines are those of westward-moving EAMDs, the yellow dots and lines are those of northwestward-moving EAMDs and the blue dots and lines are those of turning EAMDs.

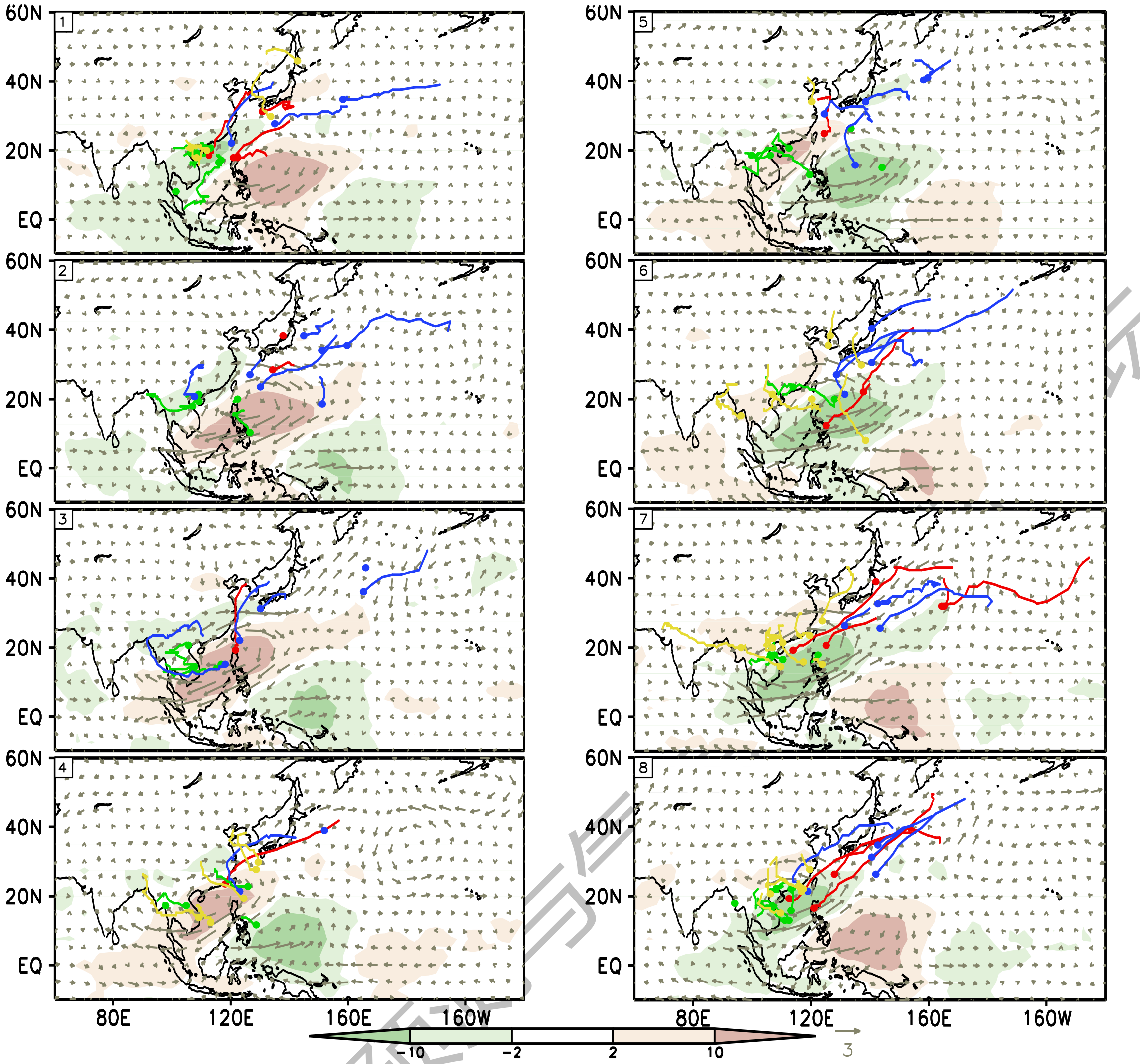

Fig. 10 Locations of peak EAMDs and tracks after the peak times (dots and lines), composite 10-20 day filtered 500 hPa anomalous winds (vectors) and OLR anomalies (shading) in the eight phases of the QBWO. The red dots and lines are the locations and tracks of eastward-moving EAMDs, the green dots and lines are those of westward-moving EAMDs, the yellow dots and lines are those of northwestward-moving EAMDs and the blue dots and lines are those of turning EAMDs.

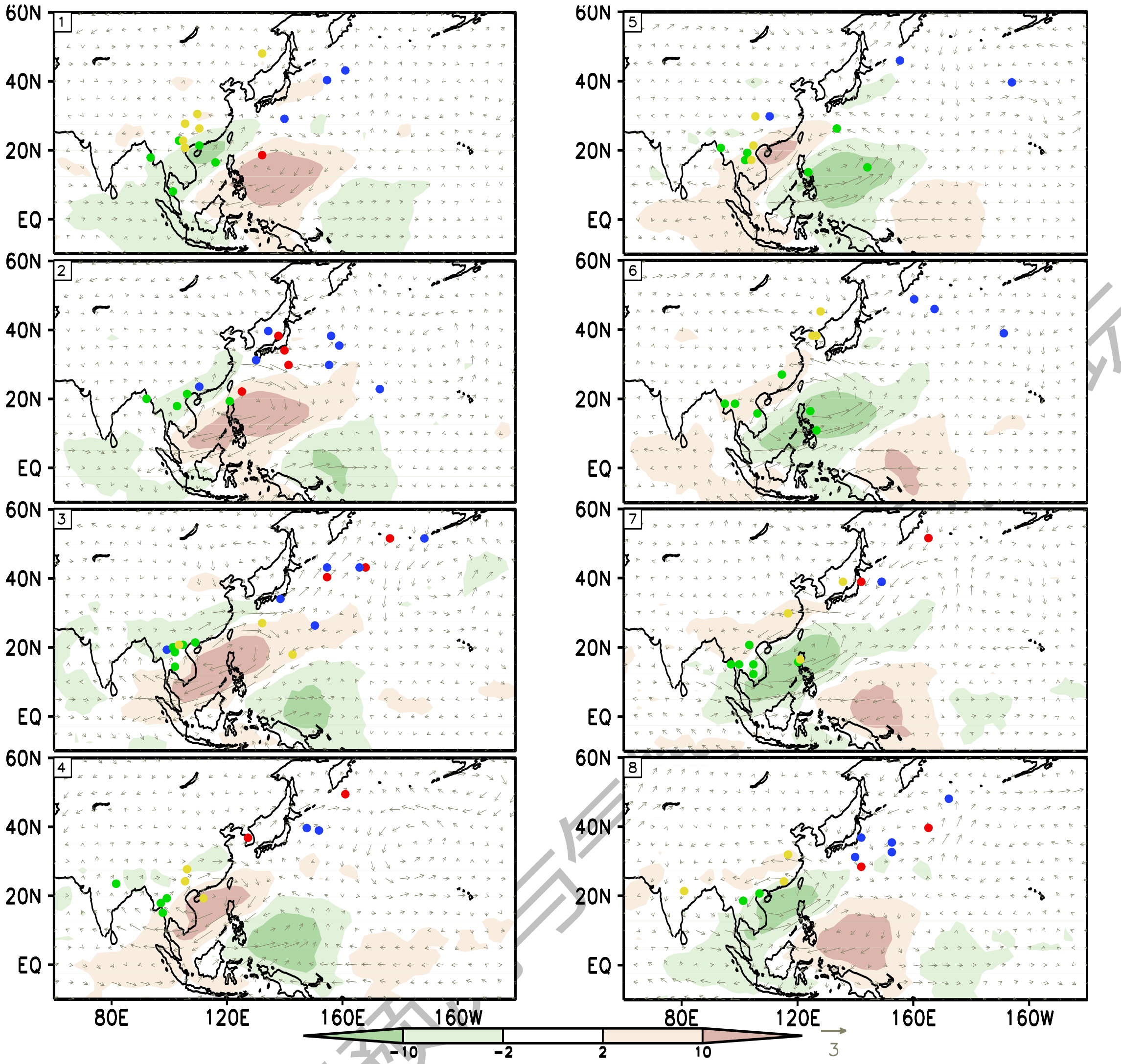

Fig. 11 Locations of the disappearance of EAMDs (dots), composite 10-20 day filtered 500 hPa anomalous winds (vectors) and OLR anomalies (shading) in the eight phases of the QBWO. The red dots are the locations of eastward-moving EAMDs, the green dots are the locations of westward-moving EAMDs, the yellow dots are the locations of northwestward-moving EAMDs, and the blue dots are the locations of turning EAMDs.

References

Chen, G. and Sui, C. H. (2010) Characteristics and origin of quasi-biweekly oscillation over the western North Pacific during boreal summer. *Journal of Geophysical Research: Atmospheres*, 115(D14). https://doi.org/10.1029/2009JD013389.

Boos, W. R., Hurley, J. V. and Murthy, V. S. (2015) Adiabatic westward drift of Indian monsoon depressions. *Quarterly Journal of the Royal Meteorological Society*, 141, 1035-1048. https://doi.org/10.1002/qj.2454.

Hurley, J. V. and Boos, W. R. (2015) A global climatology of monsoon low-pressure systems. *Quarterly Journal of the Royal Meteorological Society*, 141, 1049-1064. https://doi.org/10.1002/qj.2447.

Hu, Y., Wen, M., Li, L. and Zhang, R. (2019) Climatic characteristics of East Asian tropical monsoon depressions. *Theoretical and Applied Climatology*, 1-17. https://doi.org/10.1007/s00704-019-02835-7.

Jia, X. and Yang, S. (2013) Impact of the quasi-biweekly oscillation over the western North Pacific on East Asian subtropical monsoon during early summer. *Journal of Geophysical Research: Atmospheres*, 118, 4421-4434. https://doi.org/10.1002/jgrd.50422.

Liu, S.C. and Liang, B.Q. (1988) Probing into the Mechanism of Generation and Development of the Monsoon Depression over South China Sea. *Acta Scientiarum Naturalium Universitatis Sunyatseni*, 4, 77-88.